Mischange of a second property of the second

Nigerian Journal of Biochemistry and Molecular Biology

The Official Publication of the Nigerian Society of Biochemistry & Molecular Biology (NSBMB). Journal homepage: https://www.nsbmb.org.ng/journals/



Research Article

Virtual Screening and Elucidation of Putative Binding Mode for Small Molecule Antagonist of BCL2-BH4 Domain

Ireoluwa Y. Joel¹, Lateef A. Sulaimon^{2*}, Temidayo O. Adigun¹, Ahmeedah O. Ajibola¹, Olukayode O. Bankole³, Ugochukwu O. Ozojiofor⁴, Ifelolu A. Remi-Esan³, Aishat A. Whyte², Oluwaseun O. Taofeek², Yusuf Salami², Abosede C. Ajibare⁵

- ¹Department of Biochemistry, University of Ilorin, Ilorin Kwara state, Nigeria
- ² Directorates of Chemical Sciences, Crescent University Abeokuta, Ogun State, Nigeria
- ³ Department of Science Laboratory Technology, School of Pure & Applied Sciences, Federal Polytechnic Ilaro, Ogun state, Nigeria
- ⁴ Department of Biotechnology, Nigerian Defence Academy, Kaduna, Kaduna State, Nigeria
- ⁵Department of Biochemistry, Faculty of Basic Medical Sciences, College of Medicine, University of Lagos, Nigeria

OPEN ACCESS

ABSTRACT

* CORRESPONDENCE Sulaimon, L.L.

Sulaimon, L.L. lateef.sulaimon@cuab.edu.ng +234-802-283-5042

ARTICLE HISTORY

Received: 27/09/2024 Reviewed: 14/04/2025 Revised: 16/09/2025 Accepted: 13/10/2025 Published: 31/10/2025

CITATION

Joel, I.Y., Sulaimon, L.A., Adigun, T.O., Ajibola, A.O., Bankole, O.O., Ozojiofor, U.O., Remi-Esan, I.F., Whyte, A.A., Taofeek, O.O., Salami, Y. and Ajibare, A.C. (2025). Virtual screening and elucidation of putative binding mode for small molecule antagonist of BCL2-BH4 domain. Nigerian Journal of Biochemistry and Molecular Biology. 40(1), 48-58

https://doi.org/10.4314/njbmb.v40i1.7

Cancer cells commonly evade apoptosis, making programmed cell death a key target in therapeutic development. Central to this process is the BCL2 protein family, with the BH4 domain of BCL2 identified as critical for anti-apoptotic function. To date, Lig-BDA366 is the only known molecule that binds this domain. Seeking to discover novel BH4-binding candidates, a virtual screening of approximately one million compounds yielded 11 promising small molecules, showing binding affinities between -84 and -64 kcal/mol. Advanced computational methods-including QM-polarized docking, Induced-fit docking, and QM-MM optimization—revealed probable binding modes for the top three ligands. Lig-139068 formed interactions with GLU13, MET16, LYS17, ASP31, and GLU42; Lig-138967 interacted with ASP10, ARG12, GLU13, HIS20, MET16, and GLU42; while Lig-38831 engaged ASP10, ARG12, GLU13, LYS17, and GLU42. These molecular interactions help explain their affinity for the BH4 domain. Molecular dynamics simulations confirmed stable binding of all three ligands, although Lig-38831 showed greater flexibility than Lig-BDA366. Density Functional Theory (DFT) analysis indicated that electrophilic mechanisms may underlie the reactivity of the ligands. Altogether, these computational insights support the potential of Lig-139068, Lig-138967, and Lig-38831 as candidates for further exploration in cancer therapeutics targeting the BH4 domain

Keywords: BH4 domain of BCL2, Molecular Dynamic Simulations, BCL2-Antagonist, Apoptosis, Cancer

INTRODUCTION

The uncontrolled proliferation of cancer cells is not only driven by oncogenes but also results from defective apoptotic machinery or a combination of both (Brahmer et al., 2015; Carrizosa and Gold, 2015) as well as the development of resistance by cancer cells to chemotherapeutics-induced apoptosis. These culminate in

Copyright © 2025 Joel et al. This is an open access article distributed under the Creative Commons Attribution License CC BY 4.0, which permits unrestricted use, distribution, and reproduction in any medium, provided the original work is properly cited.

poor prognosis with an 18% overall survival rate in cancer patients (Brahmer et al., 2015). Acquired resistance to apoptotic cell death is largely due to an over-expression of anti-apoptotic genes, and down-regulation or mutation of pro-apoptotic genes (Reed, 2002). Therefore, overcoming resistance to apoptosis by activating apoptosis pathways has been a major focus in the development of therapeutic strategies for cancer treatment.

Apoptosis is an evolutionarily preserved mechanism of controlled cell deletion in nature playing a critical role such as the deletion of redundant or damaged cells in diverse

fundamental body processes of multicellular organisms (Hu et al., 2018). Its machinery consists of two major inextricably linked activation pathways: the extrinsic pathway via interaction of transmembrane receptors and death ligands (such as Fas, TNF-α, and tumor necrosis factor-related apoptosis-inducing ligand (TRAIL)) (Haggarty et al., 2003; Wang et al., 2012) and the intrinsic pathway with its consequential leakage of multiple proapoptotic proteins including cytochrome c and Smac/DIABLO from the mitochondria to the cytosol due to mitochondrial membrane potential loss (Yang et al., 2009) as well as a third, though less well-known, initiation pathway known as the intrinsic endoplasmic reticulum pathway (Haggarty et al., 2003).

The BCL2 family of proteins play major roles in the intrinsic pathway of apoptosis; the family is subdivided into two: pro-apoptosis (BH123: BAK, BAX and BH3-only proteins: BID, BIM, BAD, BIK, PUMA, and NOXA) and antiapoptosis (BCL2 protein, BCL-xL, MCL1, BCL-W, BCL-B, and BCL2a1) (Radha and Raghavan, 2017).

Briefly, the BCL2 family of proteins regulates apoptosis in the following ways: firstly, in the absence of an apoptosis stimulus, BCL2 protein (anti-apoptosis) binds with BH123 proteins: BAK and BAX (pro-apoptosis), thereby preventing activation i.e. formation of homodimers on the mitochondrion membrane. This halts the release of caspase and activation of the intrinsic apoptosis pathway (Hirotani *et al.*, 1999). However, when an apoptosis stimulus is received BH3-only proteins binds with BCL2, preventing it from interacting with BH123 protein, this process, therefore, activates the pro-apoptotic protein BAK and BAX (Hirotani *et al.*, 1999; Wang *et al.*, 2012).

The complex binding and interactions within the BCL2 family occur via their BCL2 alpha-helical homology (BH) domains (Han et al., 2015; Liu et al., 2016). There are four BH domains (BH 1- 4) of which the BH3 domain is responsible for activation and inactivation of pro-apoptosis anti-apoptosis BCL2 family proteins. overexpression of BCL2 protein has implicated in several cancerous tumors (Liu et al., 2016), the BH3 domain has been targeted for developing small molecule inhibitors of BCL2 protein (anti-apoptosis) to induce cell death in cancerous cells; inhibitors such as ABT-737, ABT-263, ABT-199, Disarib, etc. (Radha and Raghavan, 2017) have been developed with varying degrees of success (Haggarty et al., 2003; Wang et al., 2012). However, none has been approved for use; this is primarily due to the highly conserved nature of BH3 domains among the BCL2 family (Liu et al., 2016); the search for small molecules inhibitors of BCL2 protein has thus continued.

Several studies have suggested developing small molecule inhibitors targeting the BH4 domain of BCL2 protein as a potential therapeutic strategy (Hirotani *et al.*, 1999; Rong et al., 2009a; Rong *et al.*, 2009b). Han et al (2015) recently used BDA366 as a proof of concept to show the therapeutic potential in targeting the BH4 domain of BCL2 protein. The BH4 domain in BCL2 protein is important in the regulation of the anti-apoptotic activity of BCL2 protein; it is also

required in the interaction (heterodimerization) of BCL2 protein with pro-apoptosis protein BAX (Liu *et al.*, 2016). Furthermore, mutant BCL2 protein without the BH4 domain has been shown to promote apoptosis instead of inhibiting apoptosis (Rong *et al.*, 2009; Liu et al., 2016).

At the time of writing, BDA366 is the only small molecule targeting the BH4 domain that has been reported. We, therefore, sought to virtually screen for potential BH4 binding small molecules and investigate a putative binding mode for the identified compounds.

MATERIALS AND METHODS

Small molecules Library

The L sample of the SCUBIDOO database (Chevillard and Kolb, 2015) was downloaded for this study. The L sample which consists of 999,794 compounds is a sample representation of the whole database which consists of ~21,000,000 compounds.

High-throughput virtual screening Protein Preparation

Schrodinger's Protein preparation wizard (Sastry *et al.*, 2013) was used to import the BCL2 protein from PDB (PDB ID:1GM), and prepossessed: Hydrogen atoms were added, disulfide bonds were created, missing loops and side chains were added using Prime (Jacobson *et al.*, 2004) Termini was capped, water molecules beyond 5Å from het groups were deleted, finally, het sates at pH 7.0 +/- 2.0 was generated using Epik (Hu *et al.*, 2018). Hydrogen bonds in the protein structure were optimized, water molecule with less than 3 Hydrogen bonds to non-water residues/molecule was deleted, and the whole protein structure was minimized converging heavy atoms to RSMD: 0.3Å.

Ligand Preparation

The Small molecule library was prepared using Ligprep (Sastry et al., 2013). The molecule was ionized generating all possible states at pH 7.0 + /- 2.0, the ligand was desalted and tautomers were generated. Possible stereoisomers were also generated (50 per ligand).

Active site Grid generation

Using the receptor grid generation grid of the Schrodinger suit, the docking grid file was generated. However, since there is still no co-crystallized ligand in the crystal structure, we manually inputted the amino acid residues for the active sites based on information from the literature (AA 6-31) (Han et al., 2015; Liu et al., 2016)

Molecular docking

Using Schrodinger High throughput virtual screening (HTVS) workflow, the small molecule library was docked into the BH4 domain of BCL2 protein. The workflow included filtering the library based on drug and lead-likeness criteria, docking using the 3 different glide docking protocols (HTVS, SP, XP) (Shelley et al., 2007), and finally post-possessing using the Molecular Mechanics-Generalized Born Surface Area (MM-GBSA) protocol.

Molecular Mechanics-Generalized Born Surface Area

Molecular Mechanics-Generalized Born Surface Area (MM-GBSA) evaluated the binding free energies (binding affinity) and implemented geometric minimization of the docked protein-ligand complex (Singh et al., 2019). The binding free energy was calculated using the VSGB 2.0 implicit solvation model and OPLS-2005 via Prime (Lyne et al., 2006). The binding free energy is calculated using Eq.1

Δ Gbind = Gcomplex - Gprotein - Gligand (1)

GComplex, Gprotein, and Gligand represent the free binding energy of the protein-ligand complex; protein; and ligand respectively (Singh et al., 2019).

QM-Polarized Docking

QM-Polarized docking (qpld) module (Kombo et al., 2013) of Schrodinger software was used to implement the qpld experiment. It involves three steps: firstly, docking using Glide SP (Halgren et al., 2004) protocol; fifty (50) poses per ligand generated at this stage. Secondly, Quantum mechanics (QM) charges for the generated ligand poses (50 per ligand) are calculated using a semi-empirical method (Charge type: Coulson). Thirdly, redocking of ligands with new QM charges using Glide SP protocol; 20 poses per ligand is generated.

Induced-fit Docking

Induced-fit docking experiment predicted active site conformational changes and ligand binding interactions to the new conformations. Using Schrodinger induce-fit extended sampling docking protocol (Sherman et al., 2006), ligands were docked flexibly into the active site using Glide SP docking protocol (Halgren et al., 2004) with ring conformation sampled at an energy window of 2.5kcal/mol; the side chain of the active site residues was trimmed with receptor and ligand van der Waals scaling at 0.80. The maximum number of poses per ligand was set to 50. Thereafter the generated poses were refined using Prime (Jacobson et al., 2004); the residues within 5.0Å of a ligand pose were refined and side chains optimized. The refined structures within 30.0kcal/mol of the best structure and the top 20 structures overall were redocked using the Glide SP docking protocol.

QM/MM Optimization

The resulting Induced-fit docking complex was optimized using QM/MM calculations (Lopez-Blanco et al., 2014) implemented via the Schrodinger Qsite module. The ligand and side-chain residues interacting with the ligand were treated as the QM region, while the protein was treated as MM region. DFT-B3LYP and basics set 631G** level was used for the QM calculations. The MM region was treated using OPLS2005 and energy was minimized using the Truncated Newton Algorithm.

Molecular Dynamics

Molecular dynamics (MD) simulations were performed using the Desmond package (Bowers et al., 2006), and

trajectory files were visualized and assessed with Maestro (Schrödinger, 2021). Post-simulation analysis was conducted using the Simulation Event Analysis module of Schrödinger (Schrödinger, 2020) to extract key structural and dynamic properties from the trajectories.

Simulation System Parameters

The simulation system was prepared with particular attention to solvation parameters. No membrane was incorporated in the setup. Solvation was modelled using the predefined Simple Point Charge (SPC) water model. The system was enclosed within an orthorhombic simulation box, whose dimensions were determined using the buffer method with a distance of 3.0 Å along the a, b, and c axes. The box angles were maintained at 90° (alpha, beta, gamma), yielding a total box volume of 20,456 ų, with volume minimization enabled to optimize system size. No custom atomic charges were introduced. The OPLS3e force field (Harder et al., 2015) was employed throughout the system preparation and simulation stages.

For ion placement, no spatial regions were excluded. System neutrality was achieved by adding one chloride ion (Cl⁻) for the control system and four sodium ions (Na⁺) for the ligand-bound system (lig_7794). Additionally, a physiological salt concentration of 0.15 M was maintained by supplementing the system with Na⁺ and Cl⁻ ions. The OPLS3e force field (Harder et al., 2015) was consistently applied during ion addition and subsequent simulation phases.

Molecular Dynamics Production Parameters

The production MD simulations were carried out over a period of 100 nanoseconds (ns). Trajectory snapshots were recorded at 100.00 picosecond (ps) intervals, and energy data were collected every 1.2 ps, resulting in approximately 1000 frames across the simulation duration. Simulations were conducted in the isothermal-isobaric (NPT) ensemble at a temperature of 300 K and a pressure of 1.01325 bar. Prior to the production run, the system underwent relaxation following Schrödinger's standard relaxation protocol to ensure system stability.

Advanced simulation parameters included the use of the RESPA multiple time-step integrator, with time steps of 2.0 femtoseconds (fs) for bonded and near interactions and 6.0 fs for far interactions. Temperature control was achieved via the Nose-Hoover chain thermostat with a relaxation time of 1.0 ps. Electrostatic interactions were treated using the Coulombic method with a short-range cutoff distance of 9.0 Å.

Electronic Properties

In addition to classical MD simulations, quantum mechanical (QM) electronic properties were calculated using the Jaguar Single Point Energy module (Kump et al., 2020) within Schrödinger. Electronic structure calculations employed a hybrid Density Functional Theory (DFT) method, specifically using Becke's three-parameter exchange functional combined with the Lee-Yang-Parr

correlation functional (B3LYP) and the 6-31G** basis set (Bochevarov et al., 2013; Gupta, 2016). Several key electronic descriptors were derived from these calculations, including the energy gap between the highest occupied molecular orbital (HOMO) and the lowest unoccupied molecular orbital (LUMO), computed as the difference (ELUMO – EHOMO). Additional descriptors such as ionization energy (I = –EHOMO), electron affinity (A = –ELUMO), global hardness (η = (–EHOMO + ELUMO)/2), and chemical potential (μ = (EHOMO + ELUMO)/2) were also determined. Finally, the global electrophilicity index (ω) was calculated using the relationship ω = $\mu^2/2\eta$, following the framework established by Parr et al. (1999).

Mutation Analysis

Two mutant BCL2 protein structures were created and minimized: deletion of GLU42 residue (BCL2-Del) and mutation GLU42 to SER42 (BCL2-SER42): this investigated the contribution of GLU42 to the binding affinity of the ligands

RESULTS

High throughput virtual screening

In our comprehensive high-throughput virtual screening (HTVS) of 999,794 compounds, we identified a notable selection of 11 compounds with binding affinities spanning approximately -74 kcal/mol to -24 kcal/mol (Figure. 1). Among these, the control compound, BDA366, displayed a binding affinity of -45.39 kcal/mol. Subsequently, we conducted a rigorous analysis of the binding interactions for these top 11 compounds.

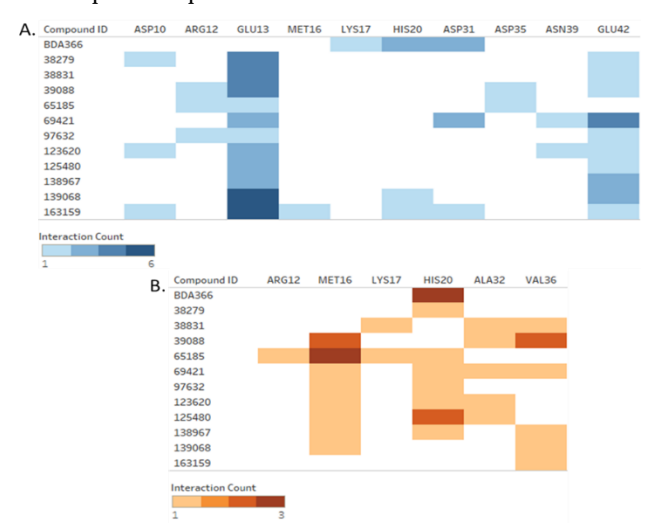


Figure 1. High throughput virtual screening binding interaction analysis: a) Hydrogen bond and electrostatic interaction count b) Hydrophobic Interaction Count.

Induced-Fit Docking

We applied the induced-fit docking protocol to determine binding modes and affinities (Figures 2-4).

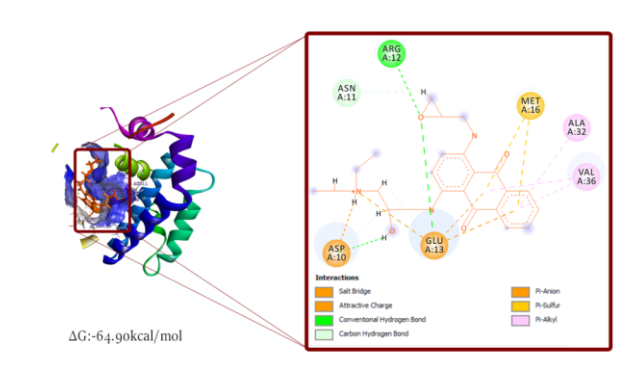


Figure 2. Induced-Fit Docking pose visualization: BDA366

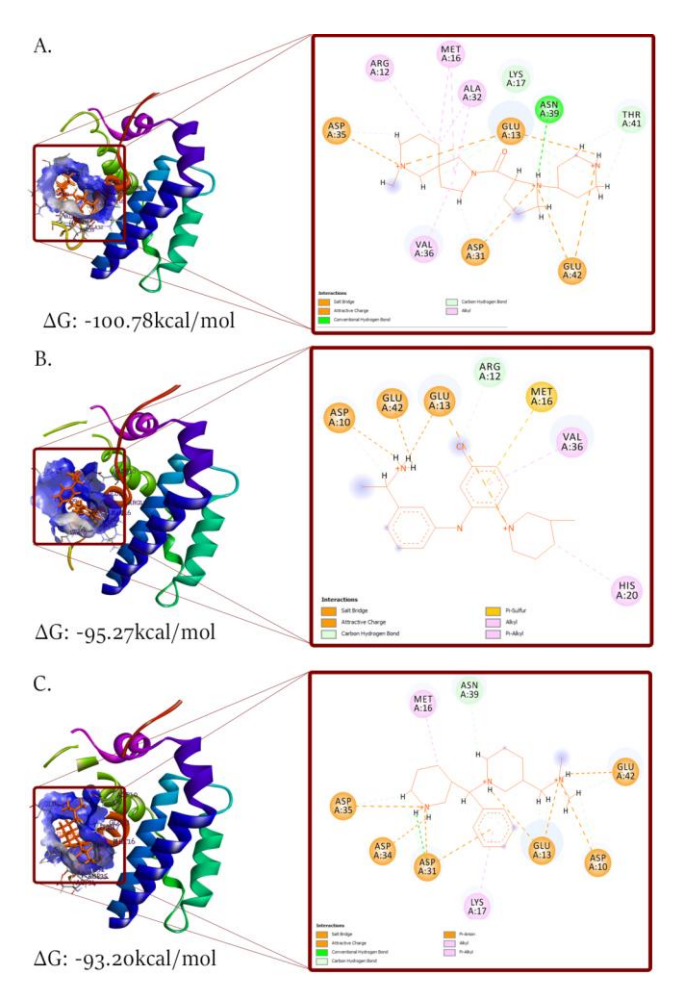


Figure 3. Induced Fit Docking pose visualization: a) 139068 b) 138967 c) 38831

Among the 11 compounds, binding affinities ranged from 100 to -85 kcal/mol. The top three compounds were 139068 (-100.78 kcal/mol), 138967 (-95.27 kcal/mol), and 38831 (-93.20 kcal/mol) (Fig. 5). Compound 139068 interacted with BH4 residues (AA: 12, 13, 16, 17, 31) and non-BH4 residues (AA: 32, 36, 41, 42). Compound 138967 interacted with BH4 residues (AA: 10, 12, 13, 16, 20) and non-BH4 residues (AA: 36, 42). Compound 38831 interacted with BH4 domain

residues (AA: 10, 13, 16, 17, 31) and non-BH4 domain residues (AA: 35, 34, 39, 42) (Figure 6).

In consolidating the binding affinities from the three different docking protocols a weighted average was calculated (Fig. 4). The weights were calculated by adding a point (1) for every interaction with a BH4 residue ("reward") and subtracting 0.5 for every interaction with non-BH4 residues ("punish"). We infer that ligand interactions with BH4 domain residues should be giving more priority and "rewarded" as the aim of this study is to identify BH4 binding molecules.

The weighted average binding affinity was calculated for the 11 compounds including BDA366 (Figure 4). Compound 139068, 138967, and 38831 were the top 3 compounds with the binding affinity of -84.46kcal/mol, -83.88kcal/mol, and -80.49kcal/mol respectively (Figure 5). These three (3) compounds were selected because they met predefined selection criteria for further analysis.

		•		
	Molecular	Qm-polarized	Induced-Fit	Weighted
Compound ID	Docking	Docking	Docking	Average
BDA366	-45.39	-49.89	-64.90	-53.40
38279	-71.97	-67.76	-85.82	-70.60
38831	-63.81	-70.95	-93.20	-83.88
39088	-66.25	-67.24	-88.43	-76.16
65185	-65.68		-87.21	-67.26
69421	-67.10	-71.73	-94.47	-74.18
97632	-64.52	-65.83	-90.49	-75.00
123620	-66.31	-66.39	-91.18	-71.75
125480	-74.67	-74.63	-88.60	-78.53
138967	-62.90	-63.90	-95.27	-80.49
139068	-67.22	-69.30	-100.78	-84.46
163159	-64.35	-64.75	-94.47	-68.82
AC (I.a., I/a., a.)				
ΔG (kcal/mol)	_			
-100.78	-45.39			

Figure 4. Ligand binding affinity for different Docking Protocol

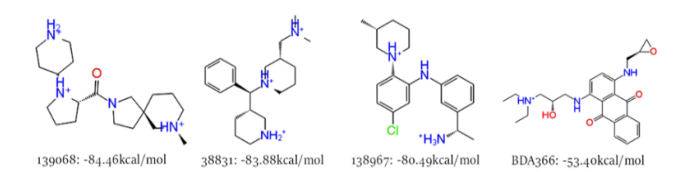


Figure 5. Top three (3) representative compounds (based on a weighted average) with BDA366 (control)

QM-MM Optimization

The molecular dynamics investigated ligand binding stability and ease of deforming the protein complex (conformational changes), Quantum mechanics - Molecular mechanics (QM-MM) calculations were used to validate ligand binding interactions. The ligand and interacting side-chain residues were treated as the QM region while the protein structure as MM region. This calculation geometrically optimized the induce-fit docking complex and validated interactions observed. Using Qsite (see methods) the QM-MM optimization was implemented, after which the binding affinity of the optimized structure was calculated using MM-GBSA. The pre-optimized pose (IFD

pose) and post-optimized pose (QM-MM pose) alongside their corresponding binding affinity were thereafter compared.

The optimized complex of compound 139068 maintained all interactions formed (when compared with pre-optimized pose) and a slight increase in calculated binding affinity (-102.15kcal/mol). Two new interactions were formed with Compound 138967: H-bond with GLU37 and electrostatic interactions with GLU38. H-bond with ARG12 was changed to hydrophobic interactions. This observed interaction changes resulted in the increase in binding affinity from -95.27 to -99.20kcal/mol (Fig. 6). Compound 38831 formed a new H-bond with THR41 and additional electrostatic interaction with ASP31. This new interaction however did not result in an increase in binding affinity but a reduction: -93.20 to -80.69kcal/mol.

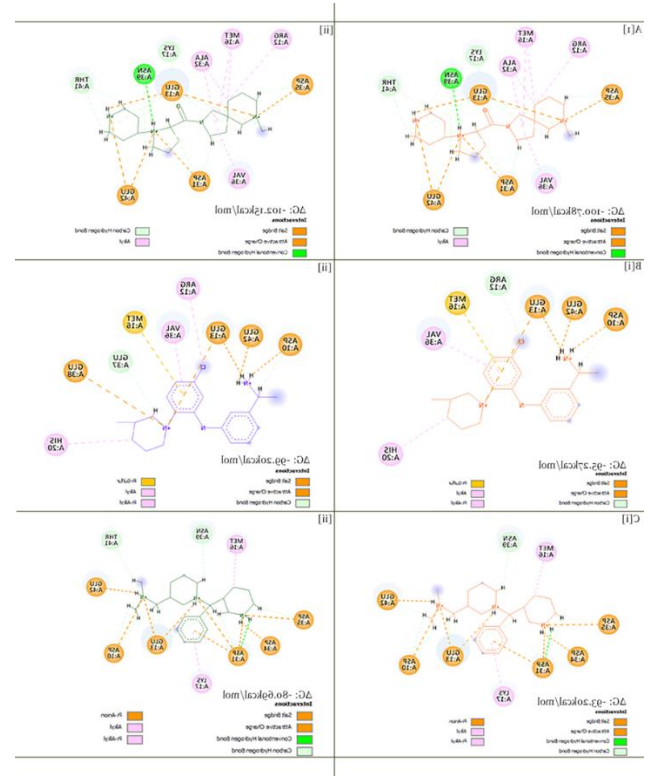


Figure 6. Comparison of pre (i) and post (ii) optimized induced-fit binding pose: a) 139068 b) 138967 c) 38831

Molecular Dynamics

Root Mean Square Deviation (RSMD)

Lig-38831 initially exhibited minimal deviation from its starting structure but quickly reached a root mean square deviation (RMSD) of approximately 0.782 Å at 49.998 ps. Following this early movement, the RMSD slightly decreased and stabilized, indicating that the ligand underwent initial conformational adjustments before settling into a relatively stable configuration. Lig-139068 displayed a similar behaviour, characterized by an initial rise in RMSD followed by a slight decline. Its deviation pattern closely mirrored that of Lig-38831, suggesting comparable stability profiles between the two ligands. In contrast, Lig-BDA366 demonstrated more dynamic

behaviour, with its RMSD increasing to 0.651 Å, rising sharply to 0.947 Å, and subsequently decreasing back to 0.651 Å. This pattern indicates greater structural flexibility relative to Lig-38831 and Lig-139068. Lig-138967 showed the highest initial RMSD value of 0.880 Å at 49.998 ps, indicating substantial early movement, followed by a continued increase in RMSD, suggesting persistent structural deviations over time.

Overall, all four ligands exhibited deviations from their initial conformations during the simulation, but Lig-138967 and Lig-BDA366 displayed more pronounced structural fluctuations compared to Lig-38831 and Lig-139068 (Fig. 7). These deviations likely reflect the ligands' conformational adaptations to their dynamic environment or the intermolecular forces acting upon them during the simulation. Higher RMSD values are indicative of greater structural rearrangements or reduced conformational stability, whereas lower and more stable RMSD trajectories suggest that the ligand structures remained relatively consistent with their initial conformations throughout the simulation period.

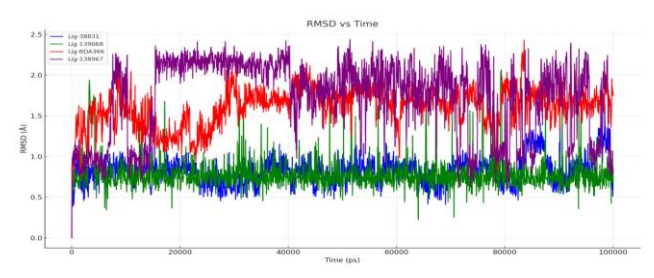


Figure 7. The RMSD of the backbone atom of BH4 domain of BCL2 after the binding of potential drug candidates

Radius of Gyration (Rgyr)

Lig-38831 began the simulation with a radius of gyration (Rgyr) value of 3.770 Å, indicating a relatively compact initial structure. Over time, its Rgyr exhibited a slight increase, suggesting minor expansion or a gradual loss of compactness; however, these changes remained modest throughout the simulation. Lig-139068 started with a larger Rgyr of 4.232 Å compared to Lig-38831, indicating a less compact initial conformation. Although its Rgyr values showed minor fluctuations during the simulation, no clear trend toward increased or decreased compactness was observed. Lig-BDA366 displayed the largest initial Rgyr at 4.463 Å, making it the least compact of the four ligands at the outset. Its Rgyr fluctuated noticeably, initially decreasing to 4.340 Å before rising again, highlighting dynamic structural changes during the simulation period. Lig-138967, starting with an Rgyr of 3.818 Å, showed a gradual decrease over time, suggesting that it became more compact as the simulation progressed.

In summary, the analysis of Rgyr values offers important insights into the size and conformational stability of the ligands throughout the simulation (Figure. 8). Lig-BDA366 exhibited the least compact starting structure and demonstrated the most dynamic behaviour, while Lig-38831

and Lig-138967 were initially more compact. Among all ligands, Lig-138967 showed a trend toward increased compactness over time, whereas Lig-BDA366 experienced significant structural fluctuations. Variations in Rgyr values can be attributed to the dynamic interactions, conformational flexibility, and environmental forces acting on the ligands during the course of the molecular dynamics' simulation.

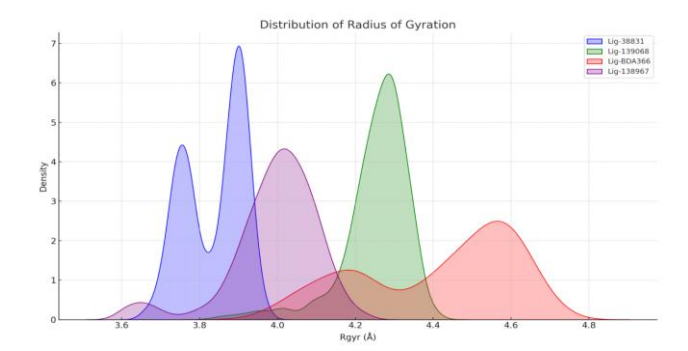


Figure 8. Distribution analysis of Rg of potential candidates

Root Mean Square Fluctuation (RMSF)

Lig-38831 exhibited a relatively high initial root mean square fluctuation (RMSF) value of 2.631 Å, suggesting considerable flexibility in certain regions of the ligand at the start of the simulation. Over time, the RMSF values fluctuated, reflecting dynamic changes in its flexibility. Around 49.998 ps, the ligand appeared to stabilize, with a reduced RMSF of 2.184 Å, although flexibility increased again in later stages of the simulation. Lig-138967, by contrast, displayed the lowest initial RMSF value of 1.216 Å, indicating greater structural rigidity compared to the other ligands. Although its flexibility varied slightly over time, Lig-138967 remained relatively stable throughout the simulation. Lig-139068 also started with a low RMSF of 0.719 Å, suggesting an initially rigid structure. Its flexibility fluctuated during the simulation but appeared to stabilize around 49.998 ps, as evidenced by a decline in RMSF values. Lig-BDA366 began with an RMSF of 2.400 Å, indicating moderate initial flexibility. Its RMSF dropped substantially to 1.484 Å at 49.998 ps, suggesting a temporary stabilization; however, it displayed considerable variability in flexibility over the course of the simulation, with RMSF values ranging between 0.756 Å and 2.562 Å.

Overall, all ligands demonstrated some degree of fluctuation in flexibility throughout the simulation (Figure. 9). Lig-38831 and Lig-BDA366 showed more pronounced dynamic behaviour, with regions exhibiting significant flexibility, whereas Lig-138967 and Lig-139068 maintained greater overall rigidity. Understanding these flexibility patterns is critical when evaluating ligand binding potential, as regions of higher flexibility may better accommodate conformational adjustments within a protein binding site, whereas highly rigid regions could limit optimal binding interactions (Figures. 10 and 11).

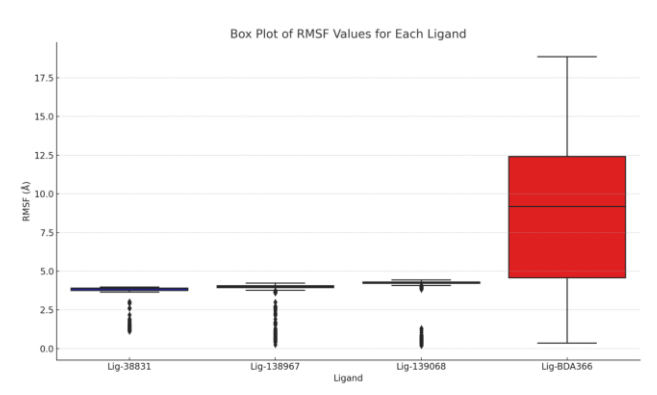


Figure 9. The root means square fluctuation (Box Plot) of the potential candidates

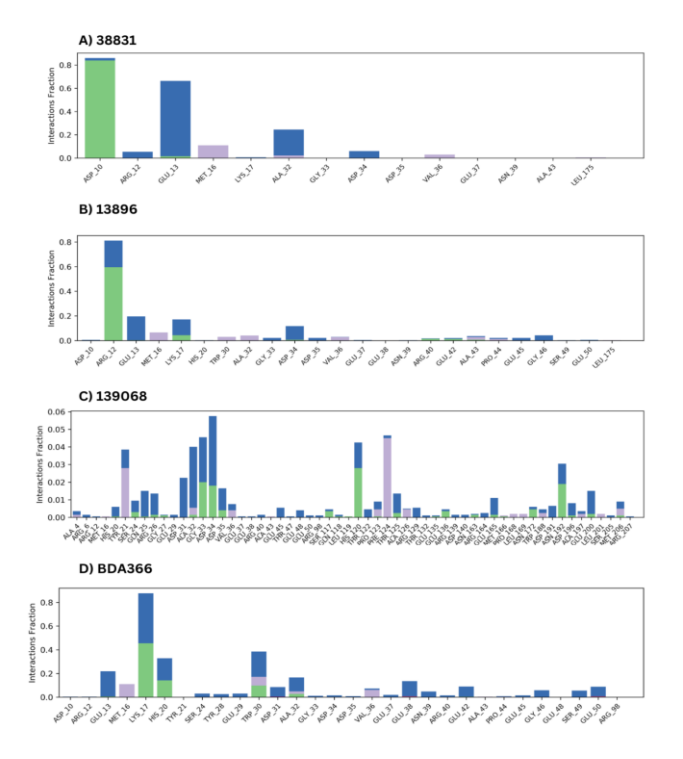


Figure 10. The binding interaction analysis of the ligands (a) 38831 (b) 13896 (c) 139068 (d) BDA366

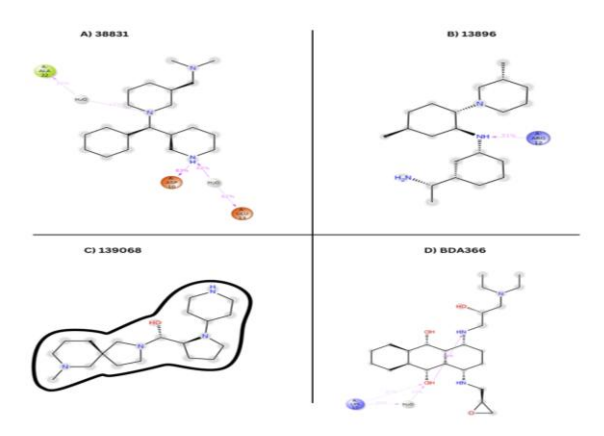


Figure 11. Visualization of the hydrogen bond interaction between protein and ligands

Electronic Properties

Electronic property (descriptors) of a ligand provides insight into how a ligand might exercise its biological activity and provides insight on how to optimize for better biological activity. Using DFT calculations implemented via Single point energy module, electronic descriptors were calculated to investigate reactivity, mechanics of reaction (electrophilic or nucleophilic reaction), and stability of the 11 compounds. The descriptors calculated include highest occupied molecular orbital (HOMO), lowest unoccupied molecular orbital (LUMO), and molecular electrostatic potential (MESP) (Figure 12); from these descriptors, the following were extrapolated: HOMO-LUMO gap, Ionization energy, Electron affinity, Chemical potential, Global hardness, and Global electrophilicity.

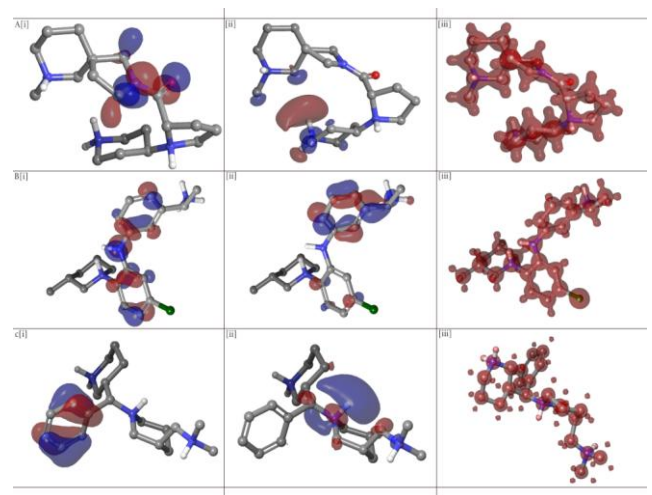


Figure 12. HOMO, LUMO, and MESP for: a) 139068 b) 138967 c) 38831

Highest occupied molecular orbital (HOMO) and lowest unoccupied molecular orbital (LUMO) are one of the most important orbitals in a compound; calculating the HOMO-LUMO gap indicates ease of electron movement (from a region of LUMO to HOMO) and stability of the compounds; a small HOMO-LUMO gap indicates a more reactive compound but less stable compound. Ionization energy is the energy required to remove an electron from a gaseous atom (it gives information about the energy of the orbital it originated from) while electron affinity is the energy change/released when an electron is added to a gaseous atom. Generally, electrons move from regions of high chemical potential to regions of low chemical potentials: therefore, a compound with low chemical potential indicates an electrophile. The Global hardness of a compound corresponds to the HOMO-LUMO gap of the compound; hardness indicates the strength electrophilicity. Global electrophilicity indicates the general reactivity of the compound. These descriptors are shown in Table 1.

Compound 123620, 69421, and 97632 appeared to be the strongest electrophiles (among the 11 compounds) with a global hardness of 0.15, however, compound 69421 was the most reactive (Global electrophilicity: -3.03). Of the three

representative compounds (139068, 138967, and 38831), compound 139068 and 38831 appeared to be the most reactive (Global electrophilicity: 0.21); however, Compound 138967 was the strongest electrophile (chemical potential: -0.34; HOMO-LUMO gap: 0.18; Global Hardness: 0.18).

Molecular electrostatic potential (MESP) of the lead compounds were calculated; it is the work done in bringing a unit positive charge from infinity to a point; it shows the surface charge distribution on the ligand thereby identify regions that might be involved in the electrophilic reaction (positively charged) and regions involved in the nucleophilic reaction (negatively charged). The MESP of the representative compounds was visualized and showed positive charge distribution on the ligand, this, therefore, confirms that the ligands interact with the BH4 domain via electrophilic reactions.

BCL2 GLU42 mutation analysis

Interaction with non-BH4 Amino acid residue GLU42 has been observed consistently with all the docking protocols and even geometric optimization (QM-MM). We, therefore, sought to investigate if interaction with GLU42 contributes directly to the binding affinity of the compounds. Two mutant BCL2 protein structures were created and minimized: deletion of GLU42 residue (BCL2Del) and mutating GLU42 to SER42 (BCL2SER42). The result showed binding affinity reduction when docked with the three representative compounds (38831, 138967, 139068) (Table 2). The data suggest that interaction with GLU42 might contribute significantly to the binding of the compounds to the BH4 domain.

Table 1. Quantum electronic descriptors of the ligands

Compound Id	HOMO (eV)	LUMO (eV)	HOMO- LUMO	Ionization energy (I)	Electron Affinity	Global Hardness	Chemical Potential	Global Electrophilicity
			GAP		(A)	(η)	(μ)	(ω)
BDA366	-0.26	-0.17	0.09	0.26	0.17	0.09	-0.22	-2.39
139068	-0.57	-0.36	0.21	0.57	0.36	0.21	-0.47	-2.21
138967	-0.43	-0.25	0.18	0.43	0.25	0.18	-0.34	-1.89
163159	-0.6	-0.32	0.28	0.6	0.32	0.28	-0.46	-1.64
38831	-0.54	-0.33	0.21	0.54	0.33	0.21	-0.44	-2.07
123620	-0.39	-0.24	0.15	0.39	0.24	0.15	-0.32	-2.10
39088	-0.53	-0.34	0.19	0.53	0.34	0.19	-0.44	-2.29
69421	-0.53	-0.38	0.15	0.53	0.38	0.15	-0.46	-3.03
97632	-0.41	-0.26	0.15	0.41	0.26	0.15	-0.34	-2.23
125480	-0.44	-0.25	0.19	0.44	0.25	0.19	-0.35	-1.82
65185	-0.34	-0.12	0.22	0.34	0.12	0.22	-0.23	-1.05
38279	-0.57	-0.33	0.24	0.57	0.33	0.24	-0.45	-1.88

Table 2. Molecular docking binding affinity of 38831, 138967 and 139068 ligands with Mutated BCL2 protein

Compound ID	BCL2	BCL2 BCL2Del	
	(kcal/mol)	(kcal/mol)	(kcal/mol)
38831	-71.97	-48.32	-58.09
138967	-62.90	-57.43	-44.19
139068	-67.22	-50.28	-55.93

DISCUSSION

The BCL2 protein, known for its role in resisting apoptosis, has been implicated in various cancer diseases (Qian et al., 2022). Consequently, numerous small molecules have been developed to counteract its activity, with most inhibitors primarily targeting the BH3 domain (Townsend et al., 2021). However, this approach faces challenges, particularly poor selectivity for BCL2, leading to the lack of FDA-approved small molecule inhibitors (Martin-Acosta and Xiao, 2021).

Addressing this, the BH4 domain of BCL2 has emerged as a promising target for converting the protein from a survival to a death protein (Martin-Acosta and Xiao, 2021). Notably, only BDA366 has been reported as a BH4-specific binding small molecule at the time of writing (Han et al., 2015). To expand the repertoire of BH4-binding molecules, virtual screening of 999,794 compounds identified 11 with a high binding affinity

(-74 to -63 kcal/mol) for the BCL2 BH4 domain, surpassing BDA366's -45 kcal/mol.

To elucidate a binding hypothesis, the top three compounds (139068, 138967, 38831) underwent rigorous docking simulations, including QM-polarized docking (QPLD) and induced-fit docking (IFD). A weighted binding affinity average consolidated results from molecular docking, QPLD, and IFD. The proposed binding hypothesis involves consistent interactions throughout all docking protocols, emphasizing the active site conformational changes considered in IFD.

The interactions of the compounds with key BH4 residues were analyzed. Compound 139068 was found to interact with GLU13, MET16, LYS17, ASP31, and GLU42; compound 138967 with ASP10, ARG12, GLU13, HIS20, MET16, and GLU42; and

compound 38831 with ASP10, ARG12, GLU13, LYS17, and GLU42. These interactions align with previous studies on BH4 residues and hydrophobic interactions (Monaco et al., 2012; Han et al., 2015).

Consistent interaction with GLU42 was observed, prompting an investigation into its role. Mutating BCL2 (deleting GLU42: BCL2Del and mutating to SER42: BCL2SER42) resulted in decreased binding affinity for the compounds, aligning with studies highlighting GLU42's role in modulating anti-apoptosis activity (Mohammadi et al., 2014; Perini et al., 2018; Qian et al., 2022).

The incorporation of molecular dynamics (MD) simulation into the examination of protein-ligand complexes following virtual screening holds considerable significance in the field of drug discovery (Duay et al., 2023). While virtual screening efficiently narrows down potential ligand candidates based on their binding affinities and complementarities, static approaches alone cannot comprehensively elucidate the dynamic behavior and intricate interactions within proteinligand complexes (Berry et al., 2015). Therefore, MD simulations play a pivotal role in unraveling the underlying dynamic intricacies that impact the stability, binding kinetics, and functional implications of these complexes (Salo-Ahen et al., 2021). This temporal dimension is particularly relevant given the inherent dynamism of biological systems. Virtual screening captures a snapshot of ligand binding, while MD simulations reveal the dynamic evolution of the complex, highlighting conformational changes and binding kinetics (Lionta et al., 2014; Mangat et al., 2022; Ahmed Maldonado and Durrant, 2023).

Molecular dynamics (MD) simulations provide a comprehensive view of the dynamic landscape of proteinligand interactions, enabling a deeper understanding of binding mode stability. By tracking key parameters such as Root Mean Square Deviation (RMSD), Root Mean Square Fluctuation (RMSF), and Radius of Gyration (Rg), researchers can evaluate the stability, flexibility, and compactness of complexes over time (Mangat et al., 2022). In the present study, MD simulations were pivotal in elucidating the dynamic behaviour, compactness, and stability of the three lead candidates, paralleling characteristics observed with Lig-BDA366. This approach aligns with findings from De Vivo et al. (2016) and Hollingsworth and Dror (2018), who emphasized that MD simulations not only predict stable binding poses but also detect conformational shifts and potential dissociation events that static methods might miss, thereby offering crucial insights into the long-term efficacy and resilience of ligand binding.

DFT calculations on electronic properties indicated potential antagonistic activities via electrophilic reactions. Compound 138967 emerged as the strongest electrophile, though not the highest binding molecule. Considering these theoretical data, including interaction with key BH4 residues, high binding affinity and stability of protein-ligand complex obtained from MD simulations as well as lower affinity for other BCL2 family proteins, compounds 38831, 139068, and 138967 are proposed as potential small molecule antagonists

targeting the BCL2 BH4 domain. However, experimental validation is needed to confirm these predictions

CONCLUSION

Targeting the BH4 domain in BCL2 protein is a promising strategy in converting the 'survival' BCL2 protein to the 'death' protein in cancer cells; identifying and developing BH4 small molecule is therefore important. Using computer simulations, 11 diverse small molecules have been identified; a binding mode for the top three (3) ligands (Lig-38831, Lig-139068 and Lig-138967) has been elucidated and the chemical reactivity of the ligands investigated. Based on our theoretical data we have suggested these three ligands as the lead antagonists of BH4 domain in BCL2 protein. However, experimental data are still needed to validate the antagonistic activity of these ligands.

AUTHORS' CONTRIBUTIONS

IYJ: Conceptualization, IYJ. LAS. and TOA.; Methodology, IYJ. and LAS.; Data curation, IYJ, LAS. and TOA.; Investigation, IYJ. LAS. and TOO.; Validation, IYJ. LAS. TOA. and UOO.; Formal analysis, AOA. OOB. and IAR; Writing-original draft, IYJ, LAS. TOA. ACA, YS. and AAW.; Writing-review and editing, IYJ, LAS, UOO. YS. and ACA. All authors have read and agreed to the published version of the manuscript.

FUNDING STATEMENT

This research did not receive any specific grant from funding agencies in the public, commercial, or not-for-profit sectors.

CONFLICT OF INTEREST

The authors declare that there is no conflict of interest

ACKNOWLEDGEMENT

Not applicable

REFERENCES

Ahmed, M., Maldonado, A. M., & Durrant, J. D. (2023). From byte to bench to bedside: Molecular dynamics simulations and drug discovery. *BMC Biology*, 21(1), 299. https://doi.org/10.1186/s12915-023-01791-z

Berry, M., Fielding, B., & Gamieldien, J. (2015). Practical considerations in virtual screening and molecular docking. In Emerging trends in computational biology, bioinformatics, and systems biology (pp. 487–502). https://doi.org/10.1016/B978-0-12-802508-6.00027-2

Bochevarov, A. D., Harder, E., Hughes, T. F., Greenwood, J. R., Braden, D. A., Philipp, D. M., ... & Friesner, R. A. (2013). Jaguar: A high-performance quantum chemistry software program with strengths in life and materials sciences. *International Journal of Quantum Chemistry*, 113(18), 2110–2142. https://doi.org/10.1002/qua.24481

Bowers, K. J., Chow, E., Xu, H., Dror, R. O., Eastwood, M. P., Gregersen, B. A., ... & Shaw, D. E. (2006). Scalable algorithms for molecular dynamics simulations on commodity clusters. In Proceedings of the ACM/IEEE

- Conference on Supercomputing (SC06), Tampa, Florida, November 11–17.
- Brahmer, J., Reckamp, K. L., Baas, P., Crinò, L., Eberhardt, W. E. E., Poddubskaya, E., ... & Mitchell, P. L. (2015). Nivolumab versus docetaxel in advanced squamous-cell non-small-cell lung cancer. *New England Journal of Medicine*, 373, 123–135. https://doi.org/10.1056/NEJMoa1504627
- Carrizosa, D. R., & Gold, K. A. (2015). New strategies in immunotherapy for non-small cell lung cancer. Translational Lung Cancer Research, 4(5), 553–559. https://doi.org/10.3978/j.issn.2218-6751.2015.06.05
- Chevillard, F., & Kolb, P. (2015). SCUBIDOO: A large yet screenable and easily searchable database of computationally created chemical compounds optimized toward high likelihood of synthetic tractability. *Journal of Chemical Information and Modeling*, 55(9), 1824–1835. https://doi.org/10.1021/acs.jcim.5b00203
- De Vivo, M., Masetti, M., Bottegoni, G., & Cavalli, A. (2016). Role of Molecular Dynamics and Related Methods in Drug Discovery. *Journal of Medicinal Chemistry*, 59(9), 4035–4061. https://doi.org/10.1021/acs.jmedchem.5b01684
- Duay, S. S., Yap, R. C. Y., Gaitano, A. L. 3rd, Santos, J. A. A., & Macalino, S. J. Y. (2023). Roles of virtual screening and molecular dynamics simulations in discovering and understanding antimalarial drugs. International Journal of Molecular Sciences, 24(11), 9289. https://doi.org/10.3390/ijms24119289
- Gupta, V. P. (2016). Density functional theory (DFT) and time dependent DFT (TDDFT). In Density functional theory (pp. 1–20). https://doi.org/10.1016/B978-0-12-803478-1.00005-4
- Haggarty, S. J., Koeller, K. M., Wong, J. C., Grozinger, C. M., & Schreiber, S. L. (2003). Domain-selective small-molecule inhibitor of histone deacetylase 6 (HDAC6)-mediated tubulin deacetylation. *Proceedings of the National Academy of Sciences*, 100(8), 4389–4394. https://doi.org/10.1073/pnas.0430973100
- Halgren, T. A., Murphy, R. B., Friesner, R. A., Beard, H. S., Frye, L. L., Pollard, W. T., ... & Shenkin, P. S. (2004). Glide: A new approach for rapid, accurate docking and scoring.
 2. Enrichment factors in database screening. *Journal of Medicinal Chemistry*, 47(7), 1750–1759. https://doi.org/10.1021/jm030644s
- Han, B., Park, D., Li, R., Xie, M., Owonikoko, T. K., Zhang, G., ... & Deng, X. (2015). Small-molecule Bcl2 BH4 antagonist for lung cancer therapy. *Cancer Cell*, 27(6), 852–863. https://doi.org/10.1016/j.ccell.2015.04.010
- Harder, E., Damm, W., Maple, J., Wu, C., Reboul, M., Xiang, J. Y., ... & Friesner, R. A. (2015). OPLS3: A force field providing broad coverage of drug-like small molecules and proteins. *Journal of Chemical Theory and Computation*, 12(1), 281–296. https://doi.org/10.1021/acs.ictc.5b00864
- Hirotani, M., Zhang, Y., Fujita, N., Naito, M., & Tsuruo, T. (1999). NH2-terminal BH4 domain of Bcl-2 is functional for heterodimerization with Bax and inhibition of apoptosis. *Journal of Biological Chemistry*, 274(29), 20415–20420. https://doi.org/10.1074/jbc.274.29.20415

- Hollingsworth, S. A., & Dror, R. O. (2018). Molecular dynamics simulation for all. Neuron, 99(6), 1129–1143. https://doi.org/10.1016/j.neuron.2018.08.011
- Hu, Y., Zhou, L., Zhu, X., Dai, D., Bao, Y., & Qiu, Y. (2018). Pharmacophore modeling, multiple docking, and molecular dynamics studies on Wee1 kinase inhibitors. *Journal of Biomolecular Structure & Dynamics*, 36(13), 3467–3480.

https://doi.org/10.1080/07391102.2018.1495576

- Jacobson, M. P., Pincus, D. L., Rapp, C. S., Day, T. J., Honig, B., Shaw, D. E., & Friesner, R. A. (2004). A hierarchical approach to all-atom protein loop prediction. Proteins: Structure, Function, and Bioinformatics, 55(2), 351–367. https://doi.org/10.1002/prot.10613
- Kombo, D. C., Grinevich, V. P., Hauser, T. A., Sidach, S., & Bencherif, M. (2013). QM-polarized ligand docking accurately predicts the trend in binding affinity of a series of arylmethylene quinuclidine-like derivatives at the $\alpha 4\beta 2$ and $\alpha 3\beta 4$ nicotinic acetylcholine receptors (nAChRs). *Bioorganic & Medicinal Chemistry Letters*, 23(17), 4842–4847. https://doi.org/10.1016/j.bmcl.2013.06.094
- Kump, K. J., Miao, L., Mady, A. S. A., Ansari, N. H., Shrestha, U. K., Yang, Y., ... & Chen, J. L. (2020). Discovery and characterization of 2,5-substituted benzoic acid dual inhibitors of the anti-apoptotic Mcl-1 and Bfl-1 proteins. Journal of Medicinal Chemistry, 63(5), 2489–2510. https://doi.org/10.1021/acs.jmedchem.9b01442
- Lionta, E., Spyrou, G., Vassilatis, D. K., & Cournia, Z. (2014). Structure-based virtual screening for drug discovery: Principles, applications and recent advances. *Current Topics in Medicinal Chemistry*, 14(16), 1923–1938. https://doi.org/10.2174/1568026614666140929124445
- Liu, Z., Wild, C., Ding, Y., Ye, N., Chen, H., Wold, E. A., ... & Ding, C. (2016). BH4 domain of Bcl-2 as a novel target for cancer therapy. *Drug Discovery Today*, 21(6), 989–996. https://doi.org/10.1016/j.drudis.2015.11.008
- López-Blanco, J. R., Aliaga, J. I., Quintana-Ortí, E. S., & Chacón, P. (2014). IMODS: Internal coordinates normal mode analysis server. Nucleic Acids Research, 42(W1), W271–W276. https://doi.org/10.1093/nar/gku339
- Mangat, H. K., Rani, M., Pathak, R. K., & Chhuneja, P. (2022). Virtual screening, molecular dynamics, and binding energy-MM-PBSA studies of natural compounds to identify potential EcR inhibitors against Bemisia tabaci Gennadius. *PLOS ONE*, 17(1), e0261545. https://doi.org/10.1371/journal.pone.0261545
- Martín-Acosta, P., & Xiao, X. (2021). PROTACs to address the challenges facing small molecule inhibitors. European Journal of Medicinal Chemistry, 210, 112993. https://doi.org/10.1016/j.ejmech.2020
- Mohammadi, M. K., Firuzi, O., Khoshneviszadeh, M. R., Razzaghi-Asl, N., Sepehri, S., & Miri, R. (2014). Derivatives: Synthesis, cytotoxic activity and molecular docking studies on B-cell lymphoma 2. *Journal of Pharmaceutical Sciences*, 2014, 1–11. https://doi.org/10.1155/2014/879308
- Monaco, G., Decrock, E., Akl, H., Ponsaerts, R., Vervliet, T., Luyten, T., ... & Bultynck, G. (2012). Selective regulation

- of IP3-receptor-mediated Ca2+ signaling and apoptosis by the BH4 domain of Bcl-2 versus Bcl-Xl. Cell Death and Differentiation, 19(2), 295–309. https://doi.org/10.1038/cdd.2011.92
- Parr, R. G., Szentpály, L. V., & Liu, S. (1999). Electrophilicity index. Journal of the American Chemical Society, 121(9), 1922–1924. https://doi.org/10.1021/ja983494x
- Pavitha, P., Prashanth, J., Ramu, G., Ramesh, G., Mamatha, K., & Reddy, B. S. V. (2017). Synthesis, structural, spectroscopic, anti-cancer and molecular docking studies on novel 2-[(anthracene-9-ylmethylene) amino]-2-methylpropane-1,3-diol using XRD, FTIR, NMR, UV-Vis spectra and DFT. *Journal of Molecular Structure*, 1147, 406–426. https://doi.org/10.1016/j.molstruc.2017.06.095
- Perini, G. F., Ribeiro, G. N., Pinto Neto, J. V., & Ribeiro, V. P. (2018). BCL-2 as a therapeutic target for hematological malignancies. *Journal of Hematology & Oncology,* 11, 65. https://doi.org/10.1186/s13045-018-0608-2
- Qian, S., Wei, Z., Yang, W., Huang, J., Yang, Y., & Wang, J. (2022). The role of BCL-2 family proteins in regulating apoptosis and cancer therapy. *Frontiers in Oncology*, 12, 985363. https://doi.org/10.3389/fonc.2022.985363
- Radha, G., & Raghavan, S. C. (2017). BCL2: A promising cancer therapeutic target. *Biochimica et Biophysica Acta* Reviews on Cancer, 1868(2), 309–314. https://doi.org/10.1016/j.bbcan.2017.06.004
- Reed, J. C. (2002). Apoptosis-based therapies. *Nature Reviews Drug Discovery*, 1(2), 111–121.

 https://doi.org/10.1038/nrd726
- Rong, Y. P., Barr, P., Yee, V. C., & Distelhorst, C. W. (2009a). Targeting Bcl-2 based on the interaction of its BH4 domain with the inositol 1,4,5-trisphosphate receptor. *Biochimica et Biophysica Acta Molecular Cell Research*, 1793(6), 971–978. https://doi.org/10.1016/j.bbamcr.2008.10.015
- Rong, Y. P., Bultynck, G., Aromolaran, A. S., Zhong, F., Parys, J. B., De Smedt, H., ... & Distelhorst, C. W. (2009b). The BH4 domain of Bcl-2 inhibits ER calcium release and apoptosis by binding the regulatory and coupling domain of the IP3 receptor. *Proceedings of the National Academy of Sciences*, 106(34), 14397–14402. https://doi.org/10.1073/pnas.0907555106

- Salo-Ahen, O. M. H., Alanko, I., Bhadane, R., & Lahtela-Kakkonen, M. (2021). Molecular dynamics simulations in drug discovery and pharmaceutical development. Processes, 9(1), 71. https://doi.org/10.3390/pr9010071
- Sastry, G. M., Adzhigirey, M., Day, T., Annabhimoju, R., & Sherman, W. (2013). Protein and ligand preparation: Parameters, protocols, and influence on virtual screening enrichments. *Journal of Computer-Aided Molecular Design*, 27(3), 221–234. https://doi.org/10.1007/s10822-013-9644-8
- Schrödinger LLC. (2020). Maestro (Release 2020-3).
- Schrödinger LLC. (2021). Maestro (Release 2022-3). https://www.schrodinger.com/products/maestro
- Shelley, J. C., Cholleti, A., Frye, L. L., Greenwood, J. R., Timlin, M. R., & Uchimaya, M. (2007). Epik: A software program for pKa prediction and protonation state generation for drug-like molecules. *Journal of Computer-Aided Molecular Design*, 21(12), 681–691. https://doi.org/10.1007/s10822-007-9133-z
- Sherman, W., Day, T., Jacobson, M. P., Friesner, R. A., & Farid, R. (2006). Novel procedure for modeling ligand/receptor induced fit effects. *Journal of Medicinal Chemistry*, 49(2), 534–553. https://doi.org/10.1021/jm050540c
- Singh, N., Villoutreix, B. O., & Ecker, G. F. (2019). Rigorous sampling of docking poses unveils binding hypothesis for the halogenated ligands of L-type amino acid transporter 1 (LAT1). *Scientific Reports*, 9, 1–20. https://doi.org/10.1038/s41598-019-51455-8
- Townsend, P. A., Kozhevnikova, M. V., Cexus, O. N. F., & Shamsuddin, S. (2021). BH3-mimetics: Recent developments in cancer therapy. *Journal of Experimental & Clinical Cancer Research*, 40, 355. https://doi.org/10.1186/s13046-021-02157-5
- Wang, L., Xiang, S., Williams, K. A., Dong, H., Bai, W., Nicosia, S. V., & Khochbin, S. (2012). Depletion of HDAC6 enhances cisplatin-induced DNA damage and apoptosis in non-small cell lung cancer cells. *PLoS ONE*, 7(5), e42813. https://doi.org/10.1371/journal.pone.0042813
- Yang, T. M., Barbone, D., & Broaddus, V. C. (2009). Bortezomib-induced apoptosis in the treatment of non-small cell lung cancer. *Journal of Internal Medicine* Taiwan, 20, 106–119. https://doi.org/10.6314/JIMT.2009.20(2).02

Publisher's Note: All claims expressed in this article are solely those of the authors and do not necessarily represent those of their affiliated organizations, or those of the publisher, the editors and the reviewers. Any product that may be evaluated in this article, or claim that may be made by its manufacturer, is not guaranteed or endorsed by the publisher. The publisher remains neutral with regard to jurisdictional claims.

Submit your next manuscript to NJBMB at https://www.nsbmb.org.ng/journals